

---

---

COMBUSTION, EXPLOSION,  
AND SHOCK WAVES

---

---

## Detailed Kinetic Mechanism of the Multistage Oxidation and Combustion of Isobutane

V. Ya. Basevich, A. A. Belyaev, S. N. Medvedev, V. S. Posvyanskii, and S. M. Frolov

*Semenov Institute of Chemical Physics, Russian Academy of Sciences, Moscow, Russia*

*e-mail: belyaev@center.chph.ras.ru*

Received April 2, 2014

**Abstract**—The aim of the study is to construct a detailed kinetic mechanism of the oxidation and combustion of isobutane, capable of describing both the high-temperature process and the multistep process at low temperatures. Isobutane was chosen because it is the first member of the homologous series of isomerized alkanes, with isooctane, a higher member of the series, exhibiting a multistage autoignition in experiment. It is shown that, under certain conditions, the autoignition of isobutane occurs in three stages, typical of normal alkanes and isooctane: cool and blue flames and a hot explosion. The proposed detailed kinetic mechanism is used to calculate the ignition delay time and laminar flame speed, with the simulation results being compared with the available experimental data. A satisfactory qualitative and quantitative agreement is observed. Autoignition during compression and an increased knock resistance of isobutane with respect to autoignition in internal combustion engines is considered. The anti-knock properties of isobutane are demonstrated to be better than those of normal butane.

**Keywords:** alkanes, kinetic mechanisms, isomers, autoignition, multistage oxidation, flame propagation

**DOI:** 10.1134/S1990793115020177

### INTRODUCTION

Based on a review of a vast body of experimental data, the author of [1] made important generalizations and introduced the concept of a multistage autoignition of hydrocarbons, with individual stages of “cool,” “blue,” and “hot” flames. The multistage autoignition manifests itself in many experiments on the oxidation of hydrocarbons [1, 2]. The literature offers a variety of detailed kinetic mechanisms (DKMs) of the oxidation and combustion of various hydrocarbons, including isomerized ones (see, e.g., [3]). However, none of the known works has shown that these mechanisms adequately describe these three stages. The only exception is the study [4]. Examining the phenomenology of the autoignition of reference fuels, such as *n*-heptane and isooctane, the authors of this work, gave the blue flame a new name, “preignition” and proposed a complex kinetic mechanism to explain its existence (involving reactions with aromatic compounds), which appears to be inapplicable to individual hydrocarbons with normal structure and their isomers.

Previously [5–12], we proposed and justified a kinetic mechanism of the blue flame, which is applicable to the normal-structure alkanes up to *n*-hexadecane. The main purpose of the present work is to develop a DKM for isobutane, which would describe as adequately as possible not only the high-temperature reactions, but also the reactions of multistage oxidation and combustion at low temperatures. Isobu-

tane was chosen because it is the first isomerized alkane and, therefore, it is reasonable to start with it to construct DKMs for such compounds. Furthermore, the objective of this work is to study (based on the developed DKM), the autoignition of isomerized hydrocarbons under compression in an internal combustion engine (ICE). The matter is that it was in ICEs that blue flames for a number of hydrocarbons were observed in the early 1950s. In experiments, the blue flame manifests itself as a preignition blue glow [2, 13, 14]; on the mixture composition–compression temperature parameter plane, blue flames are found in a region adjacent to the autoignition region. The reactions in the blue flame lead to decreases in the concentrations of fuel and oxygen and the formation of a number of intermediate and final reaction products.

Another important property of the isomerized hydrocarbons is their ability to impart a knock resistance to motor fuels: ICE gasolines may contain up to one third of isoparaffins. This feature is also considered for isobutane herein.

### CONSTRUCTION OF THE REACTION MECHANISM

To construct a multistage DKM for the oxidation and combustion of isobutane, we used the analogy method for selecting the reactions that determine the multistage nature of the process, an approach demonstrated its effectiveness in the development of the

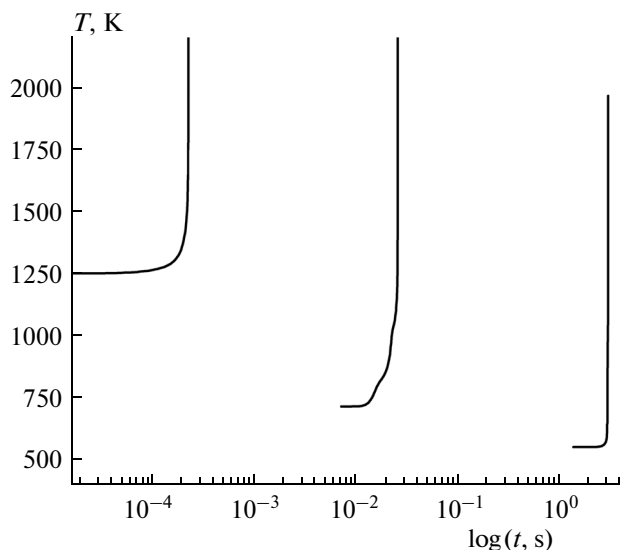


**Fig. 1.** Calculated temperature–time dependences for the autoignition of an isobutane–air stoichiometric mixture at a pressure of  $P = 19$  atm and various initial temperatures:  $T_0 = 1250, 714,$  and  $550$  K.

DKM for normal alkanes from propane to  $n$ -hexadecane [5–12]). The starting DKM was that for  $n$ -butane. It is based [6] on the principle of nonextensive construction of the mechanism, characterized by two features: it is assumed that, firstly, low-temperature branching involves a group of reactions with one oxygen addition, and, secondly, the oxidation of a normal hydrocarbon through isomeric forms can be excluded, since it is slower than the oxidation through nonisomerized components. Therefore, in constructing the DKM for isobutane  $i$ - $C_4H_{10}$ , we modified the DKM for the multistage oxidation and combustion of  $n$ -butane  $n$ - $C_4H_{10}$  [6], including blocks of reactions for hydrocarbons  $C_1$ – $C_4$ , by introducing a limited number of new components: one for each normal-structure component and probable reactions, similar to those for  $n$ -butane, that are responsible for the oxidation of isobutane. The new isomerized components in the DKM were  $i$ - $C_3H_7$ ,  $i$ - $C_3H_7O_2$ ,  $i$ - $C_3H_7O_2H$ ,  $i$ - $C_3H_7O$ ,  $i$ - $C_3H_5$ ,  $i$ - $C_4H_{10}$ ,  $i$ - $C_4H_9$ ,  $i$ - $C_4H_9O_2$ ,  $i$ - $C_4H_9O_2H$  ( $i$ - $C_4H_{10}O_2$ ),  $i$ - $C_4H_9O$ ,  $i$ - $C_3H_7CHO$  ( $i$ - $C_4H_8O$ ),  $i$ - $C_3H_7CO$  ( $i$ - $C_4H_7O$ ),  $i$ - $C_4H_8$ ,  $i$ - $C_4H_7$  (given in parentheses are compact formulas of the components in the DKM). The thermochemical parameters of isomerized components, such as the enthalpy  $\Delta H_{298}^\circ$ , entropy  $S_{298}^\circ$ , and the coefficients  $c_0$ ,  $c_1$ ,  $c_2$ ,  $c_3$ , and  $c_4$  in the expression for the heat capacity at constant pressure:  $c_p = c_0 + c_1T/10^3 + c_2T^2/10^6 + c_3T^3/10^9 + c_4T^4/10^{12}$ , were calculated based on the known recommendations and additivity rules for two intervals at low- and high-temperatures [5].

Thus, the mechanism of the oxidation and combustion of  $n$ - $C_4H_{10}$  [6] was extended to include 118 new reactions involving the 14 aforementioned isomerized components. In total, the new DKM of the oxidation and combustion of  $n$ - $C_4H_{10}$  and  $i$ - $C_4H_{10}$  includes 68 components and 409 pairs of forward and reverse reactions.

It should be noted that due the scarcity of experimental data, there is a problem of selecting the Arrhenius parameters of the rate constants for many reactions. Therefore, to construct an array of constants for the DKM of the oxidation and combustion of  $i$ - $C_4H_{10}$ , we used the parameters of similar reactions for  $n$ - $C_4H_{10}$  on the basis of the algorithm developed in [5, 6]. In this case, as in [5–12], the rate constant for the  $i$ th elementary reaction, was presented in the two-parameter form, with preexponential factor  $A_i$  and activation energy  $E_i$ ; the parameters for the isomerized components were related to those for the normal-structure components by the formulas

$$A_{i(i)} = A_{i(n)} \exp[(\Delta S_{i(i)} - \Delta S_{i(n)})/R], \quad (1)$$

$$E_{i(i)} = E_{i(n)} - 0.25[\Delta H_{i(i)} - \Delta H_{i(n)}] \quad \text{for exothermic reactions,} \quad (2)$$

$$E_{i(i)} = E_{i(n)} + 0.75[\Delta H_{i(i)} - \Delta H_{i(n)}] \quad \text{for endothermic reactions,}$$

where  $A_{i(i)}$  and  $A_{i(n)}$  are the preexponential factors in the expressions for the rate constant of the  $i$ th elementary reaction of the isomerized ( $i$ ) and normal-structure ( $n$ ) components,  $E_{i(i)}$  and  $E_{i(n)}$  are the activation energies for the  $i$ th elementary reaction involving isomerized components ( $i$ ) and normal-structure components ( $n$ ),  $R$  is the universal gas constant,  $\Delta S_{i(i)}$  and  $\Delta S_{i(n)}$  are the corresponding entropy changes in the reactions, and  $\Delta H_{i(i)}$  and  $\Delta H_{i(n)}$  are the corresponding enthalpy changes in the reactions.

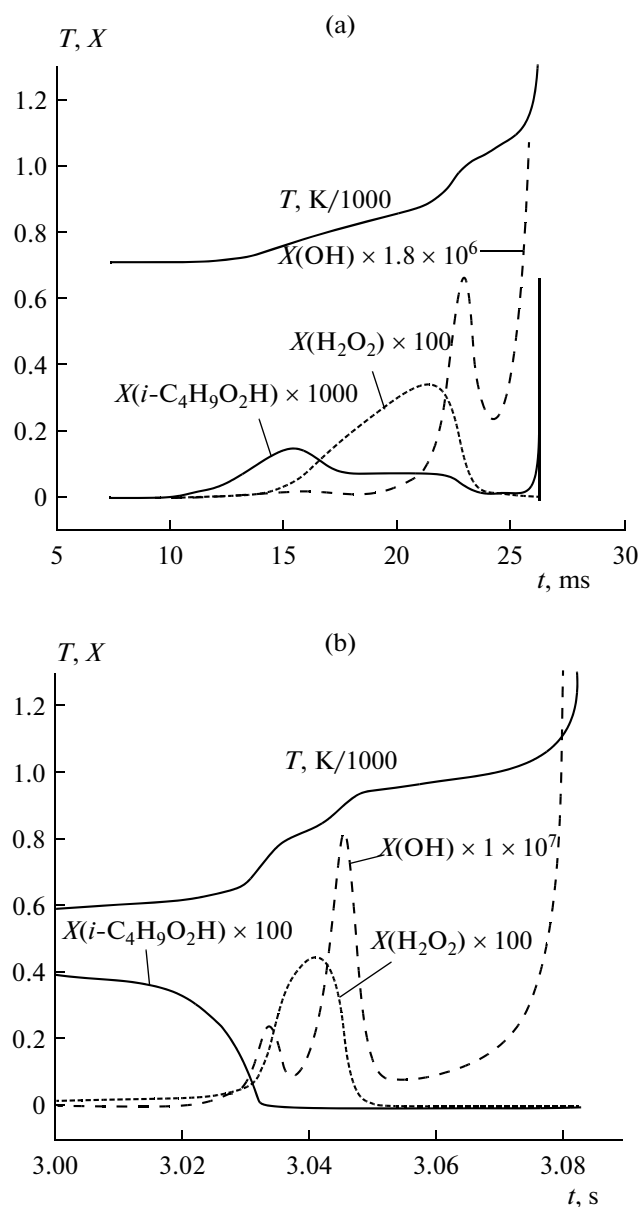
No further adjustments of thus obtained Arrhenius parameters  $A_{i(i)}$  and  $E_{i(i)}$  were performed.

## TESTING THE MECHANISM

### Autoignition

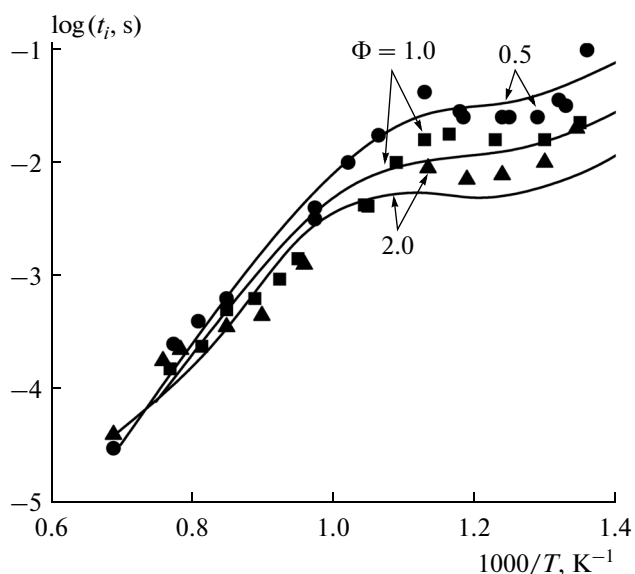
The resulting DKM was tested by comparing the results of simulation of isobutane autoignition with the available experimental data obtained on rapid compression machines and shock tubes. The calculations were performed using the code described in detail in [15].

Figure 1 shows typical calculated time histories of the temperature for the autoignition of an isobutane–air stoichiometric mixture at high (1250 K), medium (714 K), and low (550 K) initial temperatures  $T_0$  and a pressure of  $P = 19$  atm. It is seen that, at high temperature, the autoignition occurs as a single-stage process, as a two-stage at medium temperature, and again as a single-stage at low temperature, although in fact at



**Fig. 2.** Calculated time dependences of the temperature and concentrations of hydroxyl, alkyl hydroperoxide, and hydrogen peroxide for the autoignition of an isobutane–air stoichiometric mixture at a pressure of  $P = 19$  atm and initial temperatures of  $T_0 =$  (a) 714 and (b) 550 K.

medium and low temperatures, the autoignition is multistage (Fig. 2). The first stepwise rise at the initial temperature  $T_0 = 714$  K takes place at  $t \sim 0.014$  s, being associated with the occurrence of a cool flame. At  $t \sim 0.020$  s, a blue flame arises, and then, at  $t \sim 0.026$  s, a hot explosion occurs. At the initial temperature  $T_0 = 550$  K, the cool flame arises at time  $t \sim 3.035$  s, whereas the blue flame, at  $t \sim 3.045$  s. This is a manifestation of the multistage nature of the autoignition: the successive appearance of a cool and a blue flame, followed by a hot explosion. In the cool flame, the reaction accelerates due to the chain branching associated with the



**Fig. 3.** Comparison of the calculated (curves) and measured (symbols [3]) autoignition delays for  $i\text{-C}_4\text{H}_{10}$ –air mixtures at pressures of  $P = 18$ – $20$  atm and various temperatures and fuel-to-oxidizer equivalence ratios.

dissociation of the  $i\text{-C}_4\text{H}_9\text{O}_2\text{H}$  alkyl hydroperoxide to form the hydroxyl and respective oxyradical. The blue flame is associated with the branching caused by the dissociation of hydrogen peroxide ( $\text{H}_2\text{O}_2$ ) into two hydroxyls. This is confirmed by the behavior of the calculated curves for the peroxides and by two peaks in the time dependence of the hydroxyl concentration (Fig. 2). In the experiment, such a clear separation of the stages in measured time dependences of the temperature (or pressure) is not always observed because of a spatial inhomogeneity of the temperature field, but locally it is realized. Unfortunately, there is no experimental data on the hydroxyl concentration for the low-temperature autoignition.

Figure 3 compares the calculation results (curves) with the experimental data from [3] (symbols) for the autoignition of  $i\text{-C}_4\text{H}_{10}$ –air mixtures of different composition, with fuel-to-oxidizer equivalence ratios of  $\Phi = 0.5, 1,$  and  $2$  (lean, stoichiometric, and rich mixtures), at different initial temperatures and pressures of 18 to 20 atm. As can be seen, the multistage autoignition at medium and low temperatures leads to the phenomenon of a negative ( $\Phi = 2$ ), zero ( $\Phi = 1$ ), or slightly positive ( $\Phi = 0.5$ ) temperature coefficient of the reaction rate. In this case, with increasing initial temperature, the overall ignition delay time increases ( $\Phi = 2$ ), remains unchanged (at  $\Phi = 1$ ), and decreases slightly ( $\Phi = 0.5$ ). The curves calculated at different mixture compositions reflect a trend and reproduce satisfactorily the experimental data.

Figure 4 compares the calculation results (curves) with the experimental data from [3] (symbols) for stoichiometric mixtures of air with 3.11%  $i\text{-C}_4\text{H}_{10}$  and

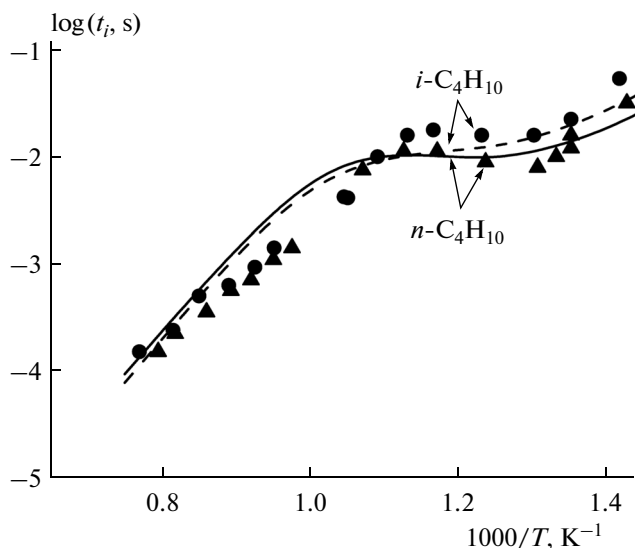


**Fig. 4.** Comparison of the calculated (curves) and measured (symbols [3]) delay times for the autoignition of stoichiometric mixtures of air with  $i\text{-C}_4\text{H}_{10}$  and  $n\text{-C}_4\text{H}_{10}$  at pressures of  $P = 18\text{--}20$  atm and various temperatures.

$n\text{-C}_4\text{H}_{10}$  at relatively high pressures,  $P = 18\text{--}20$  atm, whereas Fig. 5 shows a similar comparison with the experiments performed in [3] at high temperatures

and low pressures,  $P = 1$  and 2 atm. A satisfactory agreement is observed.

An earlier study [16] reported experimental data on the ignition delay time for  $i\text{-C}_4\text{H}_{10}$ , reduced to atmospheric pressure, which are virtually identical to the those from [3]. However, the authors of [16] additionally measured the hydroxyl concentration (Fig. 6a). Figure 6b shows the calculated hydroxyl concentration under the experimental conditions realized in [16]. The experimental and calculation results demonstrate satisfactory agreement.

#### Laminar Flame Propagation

The proposed DKM was tested by describing not only the self-ignition of mixtures of air with  $n\text{-C}_4\text{H}_{10}$  and  $i\text{-C}_4\text{H}_{10}$ , but also the propagation of planar laminar flame in such mixtures. The structure and flame speed were calculated using the method developed in [17].

Figure 7 compares the calculated and measured [18, 19] flame speed for mixtures of air with  $n\text{-C}_4\text{H}_{10}$  and  $i\text{-C}_4\text{H}_{10}$  at different compositions,  $P = 1$  atm, and  $T_0 = 293$  K. The scatter in the experimental data is large enough, comparable to the difference in the speeds of the  $n$ -butane and isobutane flames; however, the results are generally in satisfactory agreement.

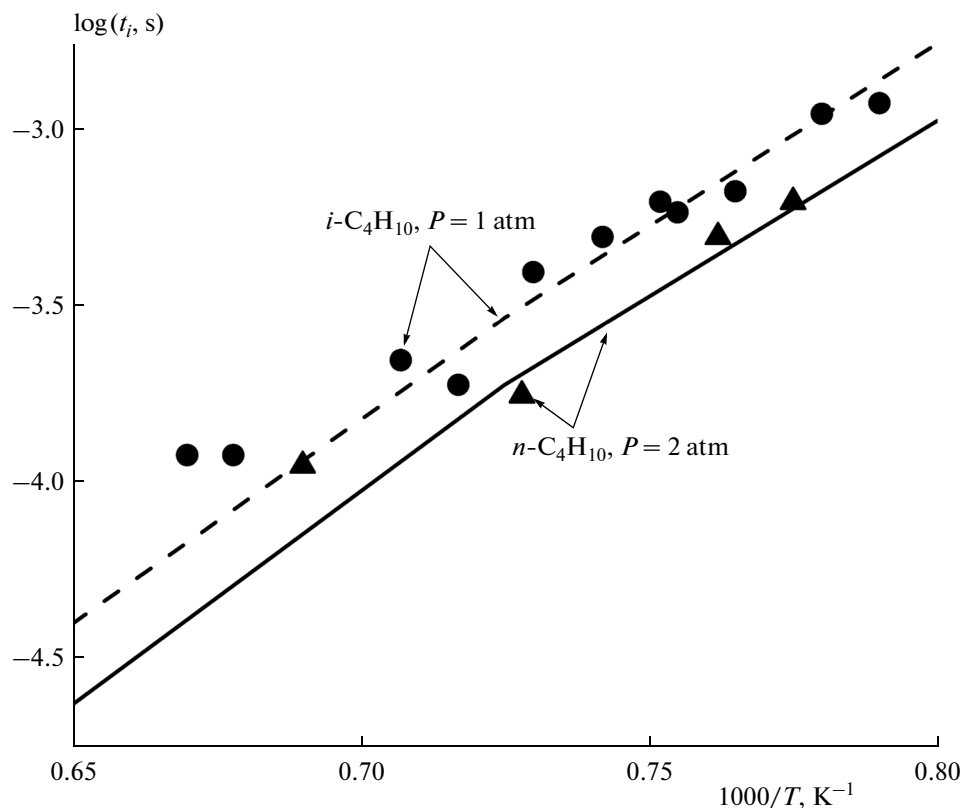


**Fig. 5.** Comparison of the calculated (curves) and measured (symbols [3]) delay times for the autoignition of stoichiometric mixtures of air with  $i\text{-C}_4\text{H}_{10}$  and  $n\text{-C}_4\text{H}_{10}$  at pressures of  $P = 1$  and 2 atm and various temperatures.

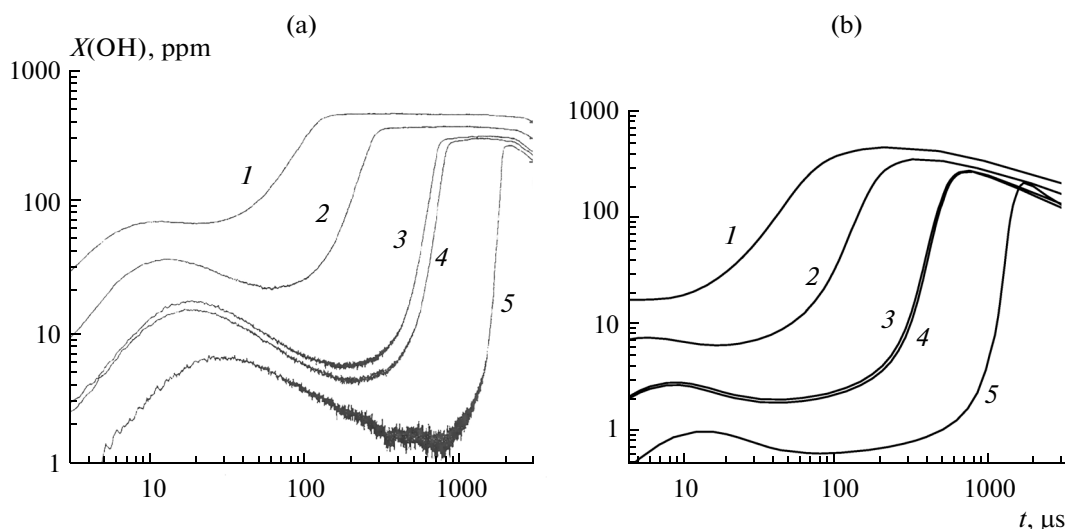


**Fig. 6.** (a) Measured [16] and (b) calculated time dependences of the hydroxyl concentration for the autoignition of a 0.1%  $i\text{-C}_4\text{H}_{10}$  + 0.65%  $\text{O}_2$  + Ar mixture at (1)  $T_0 = 1720$  K and  $P = 1.41$  atm, (2) 1593 K and 1.46 atm, (3) 1491 K and 1.50 atm, (4) 1488 K and 1.57 atm, and (5) 1411 K and 1.57 atm.

#### *Autoignition under Compression in the ICE*

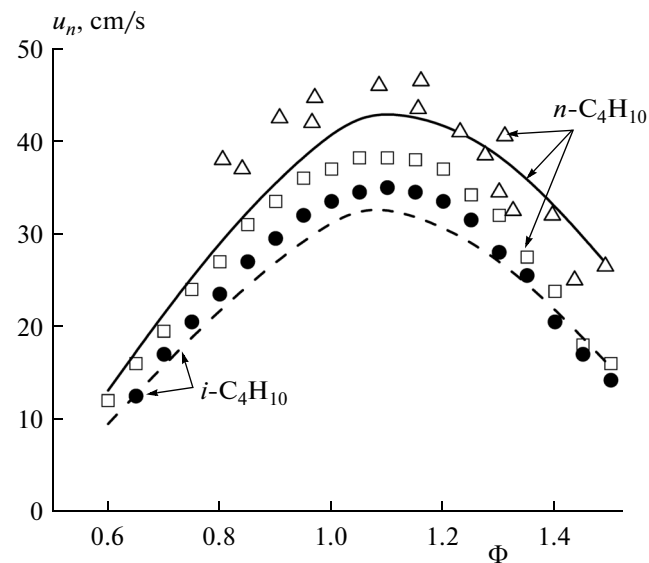
An important property of isobutane, which manifests itself during the autoignition of isobutane–air mixtures in ICEs is its knock resistance. In the present work, this property of isobutane was investigated by means of a computer program from [20], which enables to calculate the compression-induced autoignition of fuel–air mixtures in the ICE at different compression ratios  $\varepsilon$  (the ratio of the initial maximum volume of the mixture to the minimum volume at the top position of the piston). The tendency of the mixture to autoignition was analyzed by plotting the so-called indicating diagram, i.e., the dependence of the pressure on the crank angle (CA) during movement of the piston.

Figure 8 shows an example of calculating the indicating diagram for the autoignition of an isobutane–air stoichiometric mixture at  $P_0 = 1$  atm,  $T_0 = 340$  K,  $\varepsilon = 11$ , and an engine rotation speed of  $n = 600$  rpm. The calculation was performed for adiabatic conditions, i.e., without heat transfer to the cylinder walls of the gas engine. Compression begins when the piston is at bottom dead center (BDC,  $0^\circ$  CA), when the mixture occupies the maximum volume, and completes at the top dead center (TDC,  $180^\circ$  CA). In this example, the compression time was  $t = 0.05$  s ( $1^\circ$  CA corresponds to a time of  $\sim 0.278$  ms). It can be seen that the autoignition of the mixture (with multistage manifestations) begins at the TDC, while the charge burns during the stage of volume expansion (the maximum pressure and temperature are reached at a CA of  $\sim 195^\circ$ ).

Figure 9 displays the calculated time dependence of the temperature in the cylinder of the engine at different values of the compression ratio. At  $\varepsilon \sim 11$ , the mixture reacts partially during the blue flame stage,

without the occurrence of a hot explosion, whereas at higher compression ratio, the mixture ignition results in a hot explosion.

Figures 10 and 11 compare the calculated temperature–time histories (Fig. 10) and the ignition delay times  $t_i$  vs. compression ratio dependence (Fig. 11) for the stoichiometric air mixtures of  $n\text{-C}_4\text{H}_{10}$  and  $i\text{-C}_4\text{H}_{10}$ , ceteris paribus. It is seen that the anti-knock properties of isobutane are higher than those of  $n$ -butane.



**Fig. 7.** Comparison of the calculated (curves) and measured (symbols) dependences of the laminar flame speed  $u_n$  on the fuel-to-oxidizer equivalence ratio  $\Phi$  for  $i\text{-C}_4\text{H}_{10}$ –air and  $n\text{-C}_4\text{H}_{10}$ –air mixtures at  $P = 1$  atm and  $T_0 = 293$  K; experimental data from ( $\Delta$ ) [18] and ( $\square$ ,  $\bullet$ ) from [19].

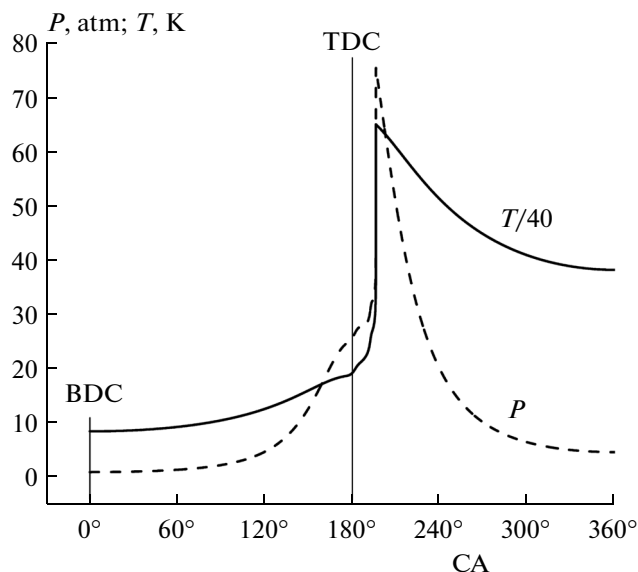


**Fig. 8.** Calculated indicating diagrams of  $P(t)$  and  $T(t)$  for the compression, autoignition, combustion, and expansion in a ICE of an  $i\text{-C}_4\text{H}_{10}$ -air stoichiometric mixture; initial pressure  $P_0 = 1$  atm, initial temperature  $T_0 = 340$  K, compression ratio  $\varepsilon = 11$ , and  $n = 600$  rpm.

In practice, fuel knock resistance is characterized by the so-called research octane number (RON), defined by means of a special technique. According to reference data, the RON for  $n\text{-C}_4\text{H}_{10}$  is  $\sim 91$ , while for  $i\text{-C}_4\text{H}_{10}$ , 99. Thus, the proposed DKM correctly predicts the knock resistance of isobutane. A relatively small difference in the RON for  $n\text{-C}_4\text{H}_{10}$  and  $i\text{-C}_4\text{H}_{10}$  explains the slight difference in experiments and calculations concerning the autoignition of  $n$ -butane and isobutane. This is in accordance with the known proposition that isomerized alkanes are more difficult to

oxidize than normal ones, since the methyl groups of isomers protect the “linear” portion of the isomerized hydrocarbon from oxidation.

## CONCLUSIONS

The conducted tests of the DKM for the oxidation and combustion of isobutane led us to conclude that the principle of nonextensive construction of the DKM with a target constraint on the variety of products and reactions, but with the preservation of the

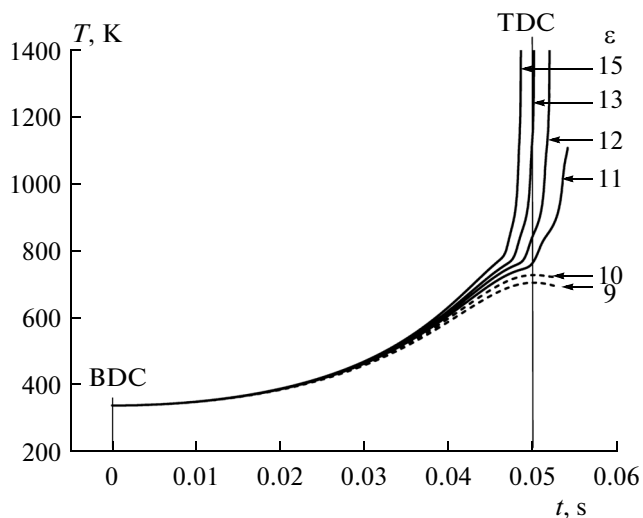


**Fig. 9.** Calculated time dependences of the temperature  $T$  at various compression ratios of a  $i\text{-C}_4\text{H}_{10}$ -air stoichiometric mixture;  $P_0 = 1$  atm,  $T_0 = 340$  K, and  $n = 600$  rpm.

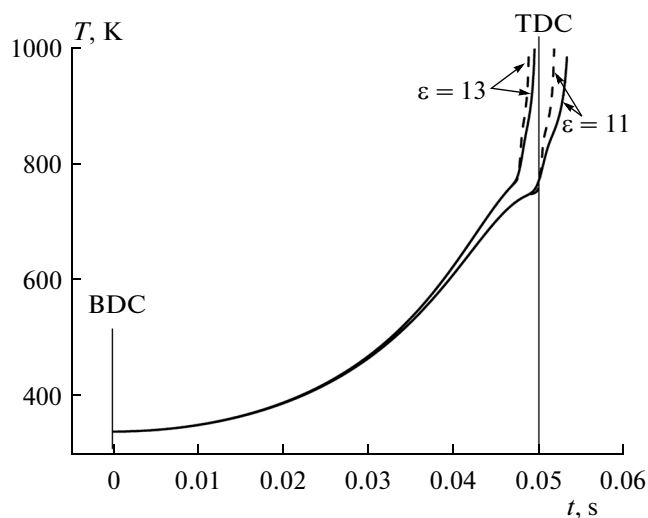


**Fig. 10.** Calculated time dependences of the temperature  $T$  for  $n\text{-C}_4\text{H}_{10}$ -air (solid curves) and  $i\text{-C}_4\text{H}_{10}$ -air (dashed curves) stoichiometric mixtures at  $P_0 = 1$  atm,  $T_0 = 340$  K,  $n = 600$  rpm, and various compression ratios.

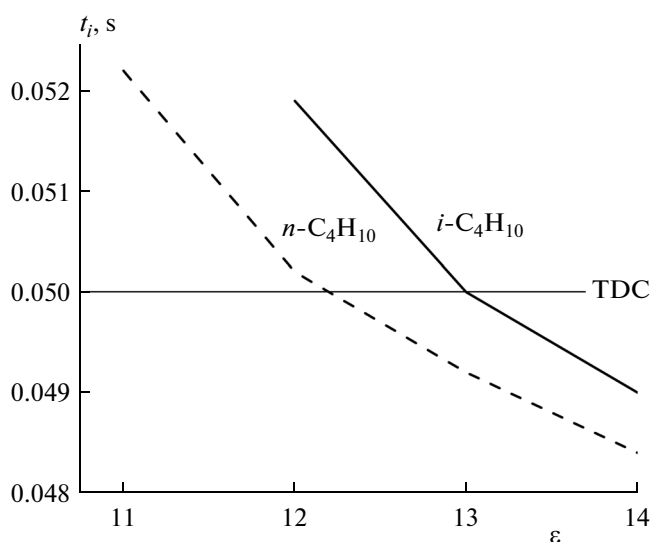


**Fig. 11.** Calculated dependences of the ignition delay time  $t_i$  on the compression ratio  $\varepsilon$  for  $n\text{-C}_4\text{H}_{10}$ -air and  $i\text{-C}_4\text{H}_{10}$ -air stoichiometric mixtures at  $P_0 = 1$  atm,  $T_0 = 340$  K, and  $n = 600$  rpm.

main channels of the process and fundamentally important types of elementary reactions, as well as the reaction kinetics obtained on its basis, are in general correct and consistent. The most important feature of the new DKM is its ability to describe the multistage nature of the process, which manifests itself in the form of cool and blue flames, followed by a hot explosion during low-temperature autoignition.

The calculated characteristics of the ignition and combustion of air-isobutane mixtures turned out to be in satisfactory qualitative and quantitative agreement with the available experimental data over wide ranges of equivalence ratio and initial temperature and pressure. The use of the proposed DKM in simulating the operation of the ICE has shown that, under certain conditions, blue flames can arise in the engine before autoignition, leading to a partial consumption of the mixture. Such phenomena were repeatedly observed in the experiment. The proposed DKM satisfactorily describes the knock propensity of isobutane and  $n$ -butane: as in the experiment, this propensity for isobutane is predicted to be better than that of normal butane.

The data file with the kinetic mechanism will be posted on the website [www.combex.ru](http://www.combex.ru).

#### ACKNOWLEDGMENTS

This work was supported by the Russian Academy of Sciences (program no. 26 "Combustion and Explo-

sion") and by the Russian Ministry of Education and Science under the state contract no. 14.609.21.0001 (contract ID RFMEFI57914X0038).

#### REFERENCES

1. A. S. Sokolik, *Self-Ignition, Flame and Detonation in Gases* (Akad. Nauk SSSR, Moscow, 1960) [in Russian].
2. A. C. Egerton, N. P. W. Moore, and W. T. Lyn, *Nature* **167**, 191 (1951).
3. D. Healy, N. S. Donato, C. J. Aul, et al., *Combust. Flame* **157**, 1540 (2010).
4. H. Machrafi and S. Cavadias, *Combust. Flame* **155**, 557 (2008).
5. V. Ya. Basevich, V. I. Vedeneev, S. M. Frolov, and L. B. Romanovich, *Khim. Fiz.* **25** (11), 87 (2006).
6. V. Ya. Basevich, A. A. Belyaev, and S. M. Frolov, *Russ. J. Phys. Chem. B* **1**, 477 (2007).
7. V. Ya. Basevich and S. M. Frolov, *Russ. Chem. Rev.* **76**, 867 (2007).
8. V. Ya. Basevich, A. A. Belyaev, and S. M. Frolov, *Russ. J. Phys. Chem. B* **3**, 629 (2009).
9. V. Ya. Basevich, A. A. Belyaev, and S. M. Frolov, *Russ. J. Phys. Chem. B* **4**, 634 (2010).
10. V. Ya. Basevich, A. A. Belyaev, V. S. Posvyanskii, and S. M. Frolov, *Russ. J. Phys. Chem. B* **4**, 985 (2010).
11. V. Ya. Basevich, A. A. Belyaev, S. N. Medvedev, V. S. Posvyanskii, and S. M. Frolov, *Russ. J. Phys. Chem. B* **5**, 985 (2011).
12. V. Ya. Basevich, A. A. Belyaev, V. S. Posvyanskii, and S. M. Frolov, *Russ. J. Phys. Chem. B* **7**, 161 (2013).
13. D. Downs, J. S. Street, and R. W. Wheeler, *Fuel* **32**, 270 (1953).
14. A. G. Gaydon, N. P. W. Moore, and J. P. Simonson, *Proc. R. Soc. A* **230**, 1 (1955).
15. B. V. Lidskii, M. G. Neigauz, V. Ya. Basevich, and S. M. Frolov, *Khim. Fiz.* **22** (3), 51 (2003).
16. M. A. Oehlschlaeger, D. F. Davidson, J. T. Herbon, and R. K. Hanson, *Int. J. Chem. Kinet.* **36**, 67 (2004).
17. A. A. Belyaev and V. S. Posvyanskii, *Algoritmy Progr., Inform. Byull. Gos. Fonda Algoritmov Programm SSSR*, No. 3, 35 (1985).
18. J. Warnatz, U. Maas, and R. W. Dibble, *Combustion* (Springer, 1996).
19. K. J. Bosschaart and L. P. H. de Goeij, *Combust. Flame* **136**, 261 (2004).
20. V. Ya. Basevich, A. A. Belyaev, A. N. Gots, V. S. Posvyanskii, I. V. Semenov, S. M. Frolov, and F. S. Frolov, in *Combustion and Explosion*, Ed. by S. M. Frolov (Nauka, Moscow, 2012), No. 5, p. 167 [in Russian].

*Translated by V. Smirnov*